Quantitative Neuroproteomics of an *In Vivo* Rodent Model of Focal Cerebral Ischemia Reperfusion Injury Reveals a Temporal Regulation of Novel Pathophysiological Molecular Markers

Arnab Datta, Qian Jingru*, Sze Hsin Khor*, Muh Tyng Teo*, Klaus Heese, Siu Kwan Sze**

* Equal contribution

** Corresponding Author

Correspondence:

Siu Kwan SZE, PhD

School of Biological Sciences, Nanyang Technological University, 60 Nanyang Drive,

Singapore 637551

Telephone: (65) 6514-1006. Fax: (65) 6791-3856. E-mail: sksze@ntu.edu.sg

Running title: Quantitative Neuroproteomics of Focal Ischemic Stroke

Keywords

Cerebral ischemia, iTRAQ, MCAO model, neuroproteomics, temporal profiling, glutamate excitotoxicity, neuroinflammation, transferrin, stroke.

SUMMARY

Cerebral ischemia or stroke, an acute neurological injury lacking an effective therapy, is the second leading cause of death globally. The unmet need in stroke research is to identify viable targets and understanding their interplay during the temporal evolution of ischemia/reperfusion (I/R) injury. Here we reported a temporal signature of the ischemic hemisphere revealed by the isobaric tag for relative and absolute quantification (iTRAQ)-based 2D-LC-MS/MS strategy in an *in vivo* middle cerebral artery occlusion (MCAO) model of focal cerebral I/R injury. To recapitulate clinical stroke, two hours of MCAO was followed by 0, 4 and 24 h of reperfusion to capture ischemia with acute and subacute duration of reperfusion injury. Subsequent iTRAQ experiment identified 2242 proteins from the ischemic hemisphere with < 1.0% false discovery rate. Data mining revealed that 1) about 2.7 % of detected proteins are temporally perturbed having involvement in the energy metabolism, glutamate excitotoxicity, neuro-inflammation, iron homeostasis and cerebral plasticity; 2) astrocytes participated actively in the neurometabolic coupling underlining the importance of a cerebro-protective rather than a neuro-protective approach; 3) the blood brain barrier (BBB) is hyperacutely yet progressively opened, accompanied by an stimulation of innate immune response and a late activation of regenerative response, provides an extended therapeutic window for intervention. Several regulated proteins (Caskin1, Shank3, Kpnb1, Uchl1, Mtap6, Epb4.1l1, Apba1, and Ube1x) novel in context of stroke was also discovered. Concluding, our result, indicating the phasic regulation of an ischemic proteome, supports a dynamic multi-target therapy rather than the traditional approach of unilateral and sustained modulation of a single target.

INTRODUCTION

Ischemic Stroke, the second most common cause of death worldwide, is a major socioeconomic burden despite decades of concerted effort to find a suitable therapy. Currently, the lone drug used in clinics, viz rt-PA (recombinant tissue plasminogen activator), is a thrombolytic agent with limited applications due to numerous exclusion criteria that includes a narrow therapeutic window of around 4.5 h [1]. Hence, the pressing need in stroke research is not only the finding of realistic targets but, more importantly, the determination of the validity of these targets during the course of temporal evolution of the disease. Failure of glutamate receptor antagonists in clinical trials was a testimony of the over-simplification of the role of glutamate in the ischemic brain as well as the hyper-acute nature of glutamate excitotoxicity in the pathological cascade of stroke [2, 3]. In addition, bi-phasic response of many proteins (vascular endothelial growth factor , Src kinase etc.), with a transition from a pro- to an anti-survival role, or vice-versa, during the evolution of the secondary injury following ischemia-reperfusion (I/R) indicates the presence of a target-specific time-window of opportunity [2-4]. Hence, a single biological marker will neither be sufficient to define this complex disease, nor will it be conducive as a therapeutic target. Thus to understand the dynamics of the molecular pathophysiology and to find potential therapeutic targets, a comprehensive temporal signature of the stroke-affected brain is needed. However, the traditional reductionist approach is not exhaustive enough to characterize multiple prospective targets temporally in a suitable *in vivo* model of cerebral ischemia.

Although recent advances in proteomics technologies offer opportunities to study the global protein landscape of various samples in a single experiment, neuroproteomics of cerebral ischemia still remains in its infancy [5]. Some of the earlier neuroproteomics studies on experimental ischemic brain samples would fall in the category of efficacy studies [6-8]. Whereas

the others, that were mechanistic in nature, were either related to ischemic preconditioning [9, 10] or used longer duration of ischemia without reperfusion [7, 11]. Spontaneous reperfusion following cerebral ischemia is clinically a well documented phenomenon [12, 13] that can lead to free radical injury apart from hemorrhagic complications [14, 15]. Recently, post-conditioning through controlled therapeutic reperfusion has gained importance in the clinical setting with the finding that uncontrolled thrombolysis can lead to reperfusion injury [16]. Thus, transient ischemia combined with an acute and sub-acute duration of reperfusion in a suitable *in vivo* model for temporal profiling offers better analogy to the clinical stroke, making it the strategy of choice to generate a panel of potential pathological makers or therapeutic targets by proteomics techniques. Most of the previous studies [8, 9, 11, 17], irrespective of their specific objectives, were technically dependent on traditional 2D-gel-based approaches (2D-GE–MS/MS) which were biased to high abundant proteins and had limited proteome coverage. A common subset of proteins (e.g. spectrin α II chain, heat shock proteins, dihydropyrimidinase-related protein 2 etc.) were identified as regulated proteins and proposed as potential pathological markers for specific events of ischemic pathophysiology.

In comparison with the gel-based methodologies, the LC-MS/MS-based multidimensional protein identification technology [18] combined with multiplex isobaric tag for relative and absolute quantification (iTRAQ) [19] provides an alternative approach for quantitative proteomics profiling. This sensitive technique allows the simultaneous quantification of proteins in 4- or 8-plex samples [20]. Recently, we have successfully applied the iTRAQ-2D-LC-MS/MS strategy for the first time in the area of cerebral ischemia to study a validated *in vitro* model of ischemic penumbra [21].To extend its application into clinically relevant *in vivo* model, we used the iTRAQ-based quantitative proteomics approach in an extra-cranial transient model of focal cerebral I/R

injury for quantitative temporal profiling of the ischemic hemisphere. First, a suitable *in vivo* model of transient focal cerebral ischemia was developed. Neurological scoring, 2, 3, 5-triphenyl tetrazolium chloride (TTC) staining and representative western blots (WB) were performed to confirm the success of the model. Subsequently the iTRAQ-based proteomics-bioinformatics platform was applied to generate a list of the pathologically important and regulated proteome from the ischemic hemisphere. Finally, some of the regulated proteins were validated at the transcriptional and translational level and were also spatio-temporally mapped by WB analysis to scrutinize deep into their functions during the evolution of cerebral I/R injury.

Our result shows for the first time the phasic regulation of several novel proteins during the course of I/R injury indicating the importance of temporally optimized therapeutic strategy to extract maximum clinical benefit.

MATERIALS AND METHODS

Reagents

Unless indicated, all reagents were purchased from Sigma-Aldrich (WI, USA).

Animals

6–8 weeks old, male Sprague-Dawley rats weighing 225–275 g were cage acclimated for 3–6 days prior to surgery in a temperature-controlled environment (24 ± 3 °C) on a 12 h light: 12 h dark cycle, with food and water *ad libitum*. Animal protocols were approved by the Nanyang Technological University Institutional Animal Care and Use Committee. Before undergoing the experimental procedures, all animals were clinically normal, free of any infection or inflammation and did not show any neurological deficits.

Induction of Cerebral I/R Injury

Focal cerebral ischemia was induced by extracranial intraluminal middle cerebral artery occlusion (MCAO) following the previously described method of Zea Longa [22] with minor modifications [23]. Details of the surgical procedure are available in Materials and Methods section of Supplemental Information (SI). Briefly, the left common carotid artery, external carotid artery (ECA) and internal carotid artery (ICA) were sequentially exposed following anesthetizing the animal. A poly-L-lysine coated 30-mm length of 3-0 polyamide monofilament non-absorbable surgical suture (Ethicon, Johnson and Johnson, USA), was inserted via ECA into the ICA till the bifurcation of left middle cerebral artery (MCA) and anterior cerebral artery to block the circulation in the left MCA territory. After 2 h of MCAO, blood flow was restored (reperfusion) by the withdrawal of the inserted suture. Sham operation was performed identically including reanesthetizing the animal after 2 h of surgery except for the brief introduction of the filament into the ECA.

Pre-Proteomics Validation

Neurological Evaluation

Post-ischemic motor and behavioral deficits were evaluated on a scale of 0–4 adopted from a previously reported neurological score with slight modifications [24]. Cumulative scoring (on a 10 (=0+1+2+3+4) point scale) was performed on all animals before and after occlusion, 1 h post occlusion, before and after reperfusion to determine the success of the surgery. Details of the neurological scoring are provided in SI Materials and Methods.

TTC Staining

TTC staining was performed to confirm the presence of infarct in the MCA territory [25]. Briefly, 2 mm think coronal sections of euthanized rat brains were placed in 1% TTC solution at 37 °C for 15 min and then fixed in buffered 4% formaldehyde solution overnight. Scion image (Alpha 4.0.3.2, Scion Corporation, Frederick, MD, USA) was used for the calculation of the infarct area using previously published formula [26]. Details of TTC staining procedure are provided in the SI Materials and Methods.

Proteomics

Experimental Design

The experimental design is depicted in Figure 1. All animals were randomly selected for age and body weight. The neurological scoring was performed by the same researcher to avoid any bias in between groups. The 2 h MCAO surgery was performed with different durations of reperfusion (n=3 for each group for proteomics analysis, i.e. biological replicate = 3 [27], 4 groups) as shown in Table 1. Sham surgery models of 2 h, 6 (=2+4) h and 26 (=2+24) h were designed to mimic the surgical trauma of I/R groups of 2+0, 2+4 and 2+24 respectively. The same sample was used for post-proteomics data validation using WB analysis. The cerebrum of the left or

ischemic hemispheres (hereafter called as ipsilateral hemisphere) was pooled from separate animals to normalize the biological and surgical variation. The olfactory lobe and cerebellum were excluded. Injection for LC-MS/MS was performed thrice (technical replicate = 3) as multiple injections give better coverage of the target proteome with superior statistical consistency. This is especially true for single peptide proteins as more MS/MS spectral evidence was obtained from multiple injections leading to higher confidence of peptide identification and quantification [28]. Validation by RT-PCR was performed in duplicate using a separate set of animals without pooling (n=2, 4 groups). Post-proteomics spatio-temporal profiling of the selected candidates from the iTRAQ-generated temporal dataset were performed on another new set of animals (n=3 for 2+0, 2+4 and 2+24, n=1 for sham).

Selection Criteria

The anesthesia duration was kept similar in all four groups (25 ± 5 min). Any animal with the surgery duration beyond the mentioned time span was excluded to avoid the differential interference of the inhalational anesthetic, isoflurene [29]. The animals showing a consistent neurological score of at least 1, 2 but not more than 3 (minimum cumulative score of 3 - 6) during the occlusion period were included for this study and randomly allocated between different groups. Animals with a lesser score were termed as ‘surgical failure’ and were excluded. The suture was withdrawn seconds before starting the trans-cardiac perfusion for animals of the ‘2+0’ group to ensure complete perfusion and to avoid any reperfusion injury. The perfused brains with a visible hematoma or hemorrhagic spot near the MCA territory or those that were not perfused properly were excluded to avoid unnecessary interference of the circulatory proteins.

Sample Preparation

The perfused ipsilateral cerebral hemispheres were obtained immediately after termination, briefly washed with PBS solution, snap-frozen in liquid nitrogen and stored at -80 °C until use. Frozen samples were homogenized with liquid nitrogen before lyses at 4 °C with ice-cold lyses buffer [2% SDS; 0.5 M triethylammonium bicarbonate (TEAB) with Complete Protease Inhibitor Cocktail (COMPLETE, Roche, Mannheim, Germany) and phosphatase inhibitor cocktail (PhosSTOP, Roche)] by intermittent vortexing and sonication (amplitude, 23%; Pulse: 5 s/ 5 s for 5 min) using a Vibra Cell high intensity ultrasonic processor (Jencon, Leighton Buzzard, UK). The lysates were centrifuged at 20 000 x g for 30 min at 4 °C. The supernatant was collected and stored in aliquots at -80 °C (longer term) or at -20 °C (shorter duration). Protein quantification was done using Bicinchoninic Acid Protein Assay kit.

In-Gel Tryptic Digestion and Isobaric Labeling

The samples were subjected to denaturing polyacrylamide gel electrophoresis (PAGE) for the purpose of removing the non-protein interfering substances. Briefly, 500 µg of protein from each condition were run on an 8% stacking–25% separating gel. Proteins which migrated into the 8% layer were retarded by the 25% layer, thus concentrating them in a narrow strip at the end of the stacking gel. The diced gel bands were then reduced (5 mM tris-(2-carboxyethyl) phosphine, 60 °C, 1 h) and alkylated (10 mM methyl methanethiosulfonate in isopropanol, room temperature, 15 min) before being digested with 10 ng/µl of sequencing-grade modified trypsin (Promega, Madison, WI) for overnight at 37 °C. The peptides were extracted with 50% ACN and vacuum centrifuged to dryness. The dried peptides were reconstituted into 0.5 M TEAB and ethanol, and labeled with respective isobaric tags of 4-plex iTRAQ Reagent Multi-Plex kit (Applied Biosystems, Foster City, CA) as follows: sham, 114; 2+0, 115; 2+4, 116; 2+24, 117 (Figure 1). The labeled samples were combined after 2 h and dried in a vacuum centrifuge.

Strong Cation Exchange (SCX) Chromatography

The dried iTRAQ-labeled peptide was reconstituted in Buffer A (10 mM KH_2PO_4; 25% ACN; pH 2.85) and fractionated using a PolySULFOETHYL A SCX column (200 × 4.6 mm; 5 µm; 200 Å) (PolyLC, Columbia) as mentioned previously [21] on a Prominence HPLC system (Shimadzu, Japan) in a 50 min gradient with Buffer B (10 mM KH_2PO_4, 25% ACN, 500 mM KCl (pH 3.0)). Eluted fractions were collected in every 1 min, and then pooled into 25 fractions, depending on the peak intensities, before drying them in a vacuum centrifuge. The dried fractions were desalted through C18 Sep-Pak Vac reverse phase cartridges (Waters, Milford, MA) and stored at -20 °C till MS analysis.

LC-MS/MS Analysis using QSTAR

The iTRAQ-labeled desalted peptides were reconstituted with 0.1% formic acid (FA) for MS analysis. Each sample was analyzed three times using a QSTAR Elite Hybrid MS (Applied Biosystems/MDS-SCIEX), coupled to an online HPLC system (Shimadzu, Japan). For each analysis, 30 µl of peptide solution was injected and separated on a home-packed nanobored C18 column with a picofrit nanospray tip (75 µm ID × 15 cm, 5 µm particles) (New Objectives, Wubrun, MA). Mobile phase A (0.1% FA in 2% ACN) and B (0.1% FA in 100% ACN) were used to establish a 90 min HPLC gradient with an effective flow rate of 0.2 µl/min, obtained from a constant flow of 30 µl/min using a splitter. The mass spectrometer was set to perform data acquisition in the positive ion mode. Precursors with a mass range of 300–2000 m/z and calculated charge of +2 to +4 were selected for fragmentation. The three most abundant peptide ions above a 5 count threshold were selected for each MS/MS spectrum. The selected precursor ion was dynamically excluded for 30 s with a 30 mDa mass tolerance. Smart information-dependent acquisition was activated with automatic collision energy and automatic MS/MS

accumulation. The fragment intensity multiplier was set to 20 and maximum accumulation time was 2 s. The peak areas of the iTRAQ reporter ions reflect the relative abundance of the proteins in the samples.

Mass Spectrometric Raw Data Analysis

The spectral data acquisition was performed using the Analyst QS 2.0 software (Applied Biosystems/MDS SCIEX). ProteinPilot Software 3.0, Revision Number: 114732 (Applied Biosystems, Foster City, CA) was used for peak list generation, protein identification and quantification against the International Protein Index rat database (version 3.40; 79354 sequences; 41861410 residues) [30]. A concatenated target-decoy database search strategy was also employed to estimate the false discovery rate (FDR) [31]. FDR was calculated the percentage of decoy matches divided by the total matches. The user defined parameters of the software were configured as described previously [21] with minor modifications (ID Focus, biological modification). The Paragon algorithm was used for the peptide identification which was further processed by Pro Group algorithm where isoform-specific quantification was adopted to trace the differences between expressions of various isoforms. The Proteinpilot software employed iTRAQ reporter ion peak area for quantification. Details of the quantification algorithm can be found in the supplier's manual. The resulting dataset were auto bias-corrected to get rid of any variations imparted due to the unequal mixing during combining different labeled samples. Subsequently background correction was also performed to eliminate any background ion signal due to non-target peptides, co-eluting with the target peptide.

Bioinformatics Analysis

Batch search was adopted by uploading the gene IDs of the proteins of interest using PANTHER 7.0 (Protein Analysis Through Evolutionary Relationships) classification system [32] against NCBI

(*Rattus norvegicus*) dataset. The regulated genes were categorized according to molecular function or biological process or protein class or pathways. Most of the genes were assigned to more than one category thus making the total number of hits greater than the number of genes uploaded.

Western Blot Analyses

WB was performed after SDS-PAGE by probing with specific horseradish peroxidase (HRP)-conjugated primary antibodies directed against proteins at the indicated dilutions: hypoxia-inducible factor-1 (Hif1a) (clone H1alpha67) 1:500 (Novus Biologicals, Littleton, CO, USA), transferrin (Tf) 1:2000 (Abcam Ltd., Cambridge, UK), heat shock protein 70 (Hsp70) 1:5000 (Abcam Ltd.), Isoform GLAST-1 of excitatory amino acid transporter 1 (Slc1a3) 1:1000 (Cell Signaling, Danvers, MA, USA), Caskin1 (1:1200) (Santa Cruz Biotech, Santa Cruz, CA, USA), vinculin (Vcl) 1:4000 , vimentin (Vim) 1:2000, glial fibrillary acidic protein (Gfap) 1:10000 (Millipore, Billerica, Massachusetts, USA), actin (Actn1) 1:4000 (clone C4) (Millipore), β-tubulin (clone B7) 1:2500 (Santa Cruz Biotech). Immunoreactivity was detected by using HRP Chemiluminescent Substrate Reagent Kit (Invitrogen, Carlsbad, CA, USA). The membranes were stained with Ponceau S and later stripped and reprobed against the actin or β-tubulin antibody to confirm uniform transfer and equal loading.

RNA Isolation and RT-PCR

Specific primers were designed by using open-source primer 3.0 software for neurofilament light polypeptide (Nefl), isoform 1 of tropomyosin alpha-3 chain (Tpm3), Gfap, Caskin1, Tf, complement C3, α-actinin or actinin1 (Actn1) (Supplemental Table 1). Total RNA was isolated using TRIzol reagent (Invitrogen) according to the manufacturer's protocol and quantified in µg/µl. Two µg of RNA was used for the reverse transcription reaction with the RevertAid H

Minus Moloney Murine Leukemia Virus Reverse Transcriptase kit (Fermentas Life Sciences, Hanover, MD, USA) following the manufacturer's instructions. Actn1 was used as internal control to check the efficiency of cDNA synthesis, PCR amplification and uniform loading. PCR products were electrophoresed through 1% agarose gels.

Spatio-temporal Profiling by Western Blot Analyses

In the MCAO model, subcortical regions (preoptic area and striatum) are first and more severely affected as a result of microvascular injury with higher chances of blood brain barrier (BBB) damage-induced edema and hemorrhagic transformation [33]. Conversely, the cortex in the transient MCAO model is affected late [12] making it suitable to study the spatial trend of the secondary injury. Thus, significantly perturbed and validated candidates from iTRAQ dataset will be selected to generate a detailed expression profile in the ischemic hemisphere. A fresh set of rats were used in triplicate for each group (except sham, where n=1) to tentatively divide the core and penumbra in this model (Figure 1, Table 1) based on our knowledge of the vascular architecture of rat brain and the TTC staining done during the model development. A 6 mm coronal section of the ipsilateral hemisphere starting 7 mm caudal to the frontal lobe was taken. It was divided into two parts, the cortical (I) containing somatosensory cortex and the subcortical (II), containing caudoputamen or striatum where part I and II represented the ischemic penumbra and core respectively.

Statistical Analysis

The physiologic variables (e.g. temperature, body weight) were presented as mean ± standard deviation (SD) to report the variability of the observations. The ordinal variable (i.e. cumulative neurological score) was presented as median ± SD. The n value indicated the number of replicate readings from same or different experiments. The possible correlation between non-parametric

variables was determined using Spearman rank correlation coefficient (time vs. cumulative neurological score). One-way ANOVA followed by post hoc Dunnett's multiple comparison test or non-parametric Kruskal-Wallis test followed by chi-square test was performed for comparing scale (physiological variables) or ordinal variables (neurological score) respectively involving at least three groups. Statistical significance was accepted at $*p < 0.05$, $**p < 0.01$.

RESULTS

Pre-proteomics Validation of the *In Vivo* Model of Focal Cerebral Ischemia

Physiological Monitoring

Rectal temperature and body weight were monitored at periodic intervals till the sacrifice of the animals. There was a statistically significant increase in weight loss at 24 h post reperfusion for stroke affected rats (11.79 ± 2.54%) in comparison with sham rats (5.22 ± 1.76%) (Table 2, Supplemental Figure 1A) due to the combined insult of intracranial and extracranial ECA territory ischemia, although the brain edema or final lesion size due to MCAO was not affected by this extracerebral ischemia [34]. Hyperthermia was observed in all the groups except sham due to the hypothalamic ischemia that peaked (38.8 ± 0.5°C) at the end of 2 h of occlusion and persisted till 24 h post reperfusion (38.2 ± 0.6°C) (Table 2, Supplemental Figure 1B) (35). Detailed result is presented in the SI Results section.

Neurological Deficits

Neurological deficit peaked at the end of 2 h of MCAO (6.0 ± 1.34), whereas progressive and partial recovery was observed spontaneously after reperfusion that persisted till 24 h (Supplemental Figure 2). This may be partly because of the use of young adult rats, a situation also encountered for younger human population with ischemic stroke [13]. Detailed result can be found in the SI Results section.

TTC Staining

The TTC staining was performed at selected time points as a part of pre-proteomics model validation that indicated the existence of the penumbra at the early time points (i.e. 2+0 and 2+4 group)(Figure 2). There was only insignificant amount of detectable necrotic tissue in the striatum at 4 h post reperfusion. The infarct spreads gradually thereafter into caudo-putamen and subsequently in the dorsolateral cortex in the next 20 h as seen in the 2+24 group [12]. Hypothalamic ischemia was also apparent in the 2+24 group as a result of 2 h of MCAO, as reported previously [35]. The overall corrected % hemispheric infarction area (%HIA) was found to be around 35% which is similar to the previously published reports [35]. The ipsilateral hemisphere at the level of bregma was the most affected one, where around 74% of the area became necrotic by 24 h of reperfusion.

Mortality

Subarachnoid hemorrhage (SAH) due to excessive insertion pressure of the intraluminal filament and inconsistency in infarct development are common drawbacks of this model necessitating the use of sufficient animals and stricter selection criteria to avoid inter and intragroup variations [36]. Post-operative mortality was around 3.6% due to SAH, whereas another 5.5% animals were excluded during autopsy due to the presence of hemorrhagic spot at the base of the brain. Another 12.7% of animals were termed as surgical failure due to an insufficient neurological score during the course of occlusion and early reperfusion probably due to premature or intermittent repefusion [36] and was excluded from the study. Thus, around 78% of the total population was progressed into the next phase for the molecular validation.

Molecular Validation by WB Analyses

Hif1a and Hsp70 were selected as representative pathological markers to complete the validation of our rat MCAO model at the molecular level [37]. The anti-apoptotic stress protein Hsp70 is generally regarded as an early response chaperone and marker of metabolic deprivation in cerebral ischemia that increases the expression of many downstream proteins as a part of the survival response [38]. In contrast, transcription factor, Hif1a is induced following a reduction in oxygen supply but not due to the inhibition of mitochondrial respiration and controls glycolysis and angiogenesis in the ischemic brain. During the entire 26 h (2 + 24 h) of I/R experiment the increased expression of Hsp70 and the transient upregulation of Hif1a (with a peak at 4 h of reperfusion) compared with the sham hemisphere (Figure 3) indicated the specific stress response by the viable cells confirming the success of our rat I/R model.

Proteomics

Group allocation for the proteomics experiments were finalized after development of the MCAO model of cerebral I/R injury in the abovementioned pilot studies using neurological scoring, TTC staining and WB analysis as shown in Figure 1.The animals were carefully screened to comply with the selection criteria for including them in the proteomics, post-proteomics validation and spatio-temporal profiling experiment. The groups were similar ($p > 0.05$, one way ANOVA) with respect to the measureable parameters like pre-operative body weight or rectal temperature (Supplemental Table 2) and pre- or post-ischemic cumulative neurological score (data not shown).

iTRAQ Results

To understand the global proteomics changes that occurred in the ipsilateral hemisphere at different time-points, pooled protein extracts from each group (n=3, biological replicate) were labeled and analyzed as described in the experimental procedure. Three technical replicates were

compared and combined to ensure the quality of the dataset and to ensure instrumental reproducibility. Details of the replicates are provided in the Supplemental Data A and B. The ProteinPilot software generated protein and peptide summary of the combined dataset are provided in the Supplemental Data C and D.

Quality Control of iTRAQ Dataset

To minimize the false positive identification of proteins, a strict cutoff of unused ProtScore ≥ 2 was used as the qualification criteria, which corresponds to a peptide confidence level of 99%. With this criterion, 2242 proteins were identified with a FDR of 0.33% (<1.0%) (Supplemental Data A and C). The average number of unique peptides (having a confidence level of >95%) detected per protein was 9.23 and 37% of the proteins had ≥ 5 unique peptides which was similar to our recently published report [21] (Supplemental Data C). The ratios for each condition were sorted using a *p*-value cut-off of 0.05 to obtain the list of proteins with significant ratios. The *p*-value in the protein pilot software helps to assess whether the observed changes in proteins' expression are real or not. It allows the results to be evaluated based on the certainty of a change in expression but not just by the magnitude of the change.

Estimation of Cutoff for Confidently Defining Perturbed Proteins

Next, the cut-off for up- or down-regulation was determined based on the analytical variation between three technical replicates as previously reported with slight modifications [21, 39]. The bias and background corrected datasets from the individual replicates were taken after removing the low confident proteins (unused score < 2.0). A total of 1166 proteins were found to be common among three technical replicates having quantification information for all iTRAQ labels. Subsequently, Geometric mean and ratio-specific (2+0: sham, 115:114; 2+4: sham, 116:114; and 2+24: sham, 117:114) standard deviation were calculated using $\log_{10}$ space for all the proteins

using triplicate values from three MS runs (Supplemental Data B). The average standard deviation in log space was 0.086, 0.080 and 0.080 for three ratios. The frequency histogram and corresponding cumulative (%) was plotted (Supplemental Figure 3) for all three ratios (115:114, 116:114 and 117:114) to measure distribution of the variation. About 93% and 99.2% of the commonly quantified proteins had a standard deviation lesser than 0.2 and 0.4 respectively among technical replicates. Based on this, the regulation cut-off was set at 1.4 fold; ratio >1.40 or <0.71 was considered as up- or down-regulated.

Subsequently, the final list of regulated candidates was obtained separately for each time-point by applying the *p*-value and regulation cut-off. Thus, 24, 28 and 37 proteins from 2+0, 2+4 and 2+24 group (having overlap between different time-points) respectively showed significant perturbation with a magnitude beyond the specified cut-off of 1.4 fold. When combined to list the unique proteins by abiding all the criteria, only 61 candidates (2.72 % of total hits) remained having at least one significant ratio ($p < 0.05$) with the expression level > 1.40 or < 0.71 (Supplemental Table 3A). This dataset was advanced to the next phase for rigorous validation by complementary techniques.

Post-proteomics Validation of the Regulated Protein dataset by WB and RT-PCR

Result validation was performed by WB with the same pool of protein extracts from the iTRAQ experiment and by RT-PCR using another independent I/R experiment done as duplicate (Figure 1).

Direct Validation of the iTRAQ Dataset by WB Analyses

WB analyses were used as a direct approach to verify the expression trends shown by the iTRAQ experiment. Six proteins (i.e. Tf, Slc1a3, Caskin1, Vim, Vcl and Gfap) out of 61 candidates representing distinct events in the pathology of ischemic stroke were chosen from the dataset. Tf is a circulatory protein whereas Slc1a3 (excitatory amino acid transporter) is an astrocyte-

specific membrane-bound high-affinity sodium-dependent aspartate/glutamate transporter. Three intermediate filament-related structural proteins (Gfap, Vim and Vcl) were chosen as they may be representative of the neurorestorative response in the ischemic brain. Actn1 was used as house-keeping control as the iTRAQ dataset showed no alterations at all time points. As seen in Figure 4 and Table 3, WB showed similar trends with the corresponding iTRAQ ratios.

Indirect Validation of iTRAQ dataset by RT-PCR

RT-PCR was also performed to check whether the regulation was at the level of transcription or due to post-transcriptional control that actually determined the net expression level. Genes corresponding to six regulated proteins (C3, Tf, Tpm3, Nefl, Gfap and Caskin1) were selected apart from Actn1 which was used as the housekeeping control. Except Tf, all other genes showed similar trends corresponding to their protein expression levels seen in the iTRAQ dataset.

Temporal Regulation of Perturbed Proteins following Focal Cerebral I/R Injury

The gene IDs of the significantly regulated proteins from the filtered and validated dataset were classified by PANTHER 7.0 using 'pathway' as ontology. They were assigned to 18 different pathways (Supplemental Table 4). 14.2% and 14.3% of the gene hit against total pathway hits were associated with glucose metabolism (7.1% each for ATP synthesis and glycolysis) and glutamate neurotransmission (7.1% for the ionotropic glutamate receptor pathway and 3.6% each for the metabotropic glutamate receptor group III pathway and glutamine/glutamate conversion) respectively. Blood coagulation (14.3%), inflammation (3.6%) and angiogenesis (3.6%) were featured among the other perturbed pathways that was consistent with the vascular nature of this disorder. Strikingly, a few of the regulated genes (Ubiquitin carboxyl-terminal hydrolase isozyme L1 (Uchl1), Amyloid beta A4 precursor protein-binding family A member 1 (Apba1), cytoplasmic dynein 1 heavy chain 1 (Dync1h1)) were also assigned to various chronic

neurodegenerative disorders (e.g. Parkinson disease, Alzheimer disease (AD) and Huntington disease). Guided by the above trends, regulated proteins were manually classified (Table 3) with incorporation of additional candidates based on their identification information only (Supplemental Table 3B) considering their association with the regulated proteins (see discussion).

Sustained upregulation of energy metabolism related proteins following I/R injury signified an adaptive response of the stressed brain that includes glycogen mobilization (brain glycogen phosphorylase (Pygb)) to glycolysis (phosphoglycerate kinase 1 (Pgk1), phosphoglycerate mutase 1 (Pgam1) etc.) and oxidative phosphorylation (ATP synthase subunit beta, ATP synthase subunit alpha). Early upregulation was seen for two glial glutamate transporters (Slc1a3 and Isoform Glt-1A of excitatory amino acid transporter 2 (Slc1a2)) having a neuroprotective role in the glutamate-mediated excitotoxicity [40]. Persistent increase in glutamine synthetase (Glul), an enzyme with almost exclusive astrocytic localisation, and significant upregulation of glutamate dehydrogenase 1 (Glud1) were observed after 2 h of ischemia. The significant presence of several acute phase proteins after 2 h of ischemia (Figure 6A) indicated an hyperacute opening of the BBB as reported recently [41]. All candidates of this group except beta-1 subunit of hemoglobin (Hbb) showed an ascending trend of absolute expression indicating progressive neuroinflammation and vasogenic edema as a result of I/R injury. The precipitous elevation in the overall expression of albumin can be explained by the complementary de novo expression in the ischemic hemisphere when albumin mRNA and protein expression was elevated after 2 h of MCAO and 22 h of post reperfusion [42]. To evaluate the de novo component on the overall expression of the plasma-derived candidates, C3 and Tf were chosen as representatives and their expression level was checked at the transcript level. Increased mRNA

level of C3 after 24 h proved the participation of brain cells in complement generation that is most likely supplemented by the massive infiltration of circulatory leukocytes and direct leakage of C3 from the circulation. The absence of mRNA regulation for Tf confirmed its circulatory source as a result of a progressive destruction of the BBB.

Significant decrease in the levels of essential structural and cytoskeletal proteins (e.g. Myosin-10 (Myh10), Plectin 3 (Plec1), Dync1h1, and Spectrin beta chain, brain 2 (Spnb3)) was observed 2 h after MCAO. All of them recovered while some others showed significantly increased level (e.g. Gfap, Vim, Vcl, etc.) at the end of 24 h of reperfusion indicating the presence of cerebral plasticity in the ischemic brain. This may be a part of the endogenous recovery response happening in parallel with the worsening of the secondary injury as exhibited by the generalized downward trend of the synapse related proteins, the other subclass under the category of "cerebral plasticity", (Figure 6B) till 24 h of reperfusion. Nevertheless, the regulated list also consisted of several regulated proteins (e.g. Caskin1, Isoform 1 of SH3 and multiple ankyrin repeat domains protein 3 (Shank3), Apba1, Catenin delta-2 (Ctnnd2), Ubiquitin-activating enzyme E1 (Ube1x), Importin subunit beta-1 (Kpnb1) etc.) novel in context of the pathophysiology of cerebral ischemia proving the utility of this discovery approach. For example, Imporins are involved in the signal mediated and energy-dependent selective import of macromolecules (transcription factors and kinases) from cytosol to nucleus. Seizure induced increase in Kpnb1 has been observed in rat hippocampus arising from the chondroitin sulfate proteoglycan neuron/glial antigen 2 expressing cells, a glial subtype recently shown to regulate hippocampal neuron excitability [43]. Thus, a biphasic response by Kpnb1 and Ipo7 (predicted importin 7) may be partly related to pathologic alterations in glutamate neurotransmission, a condition shared by ischemic stroke and seizure.

Spatio-temporal Profiling of the Validated Candidates

Two of the validated candidates (Tf and Gfap) from the iTRAQ dataset, representing two distinct events of stroke pathophysiology (Table 3) were chosen to define this model by spatio-temporal profiling. As seen from Figure 7, the presence of Tf peaked at 4 h in the core (part II) followed by a plateau or decrease at 24 h, whereas for part I, a gradual but detectable increase with time was observed as inflammation and vasogenic edema spreads into the penumbral area. The well studied astrocytic marker Gfap showed an increasing trend in the penumbra (part I) and recovered from an early decrease in the core at 24 h post I/R injury, confirming the reactive gliosis in the MCA territory.

DISCUSSION

The fundamental mechanisms that orchestrate the cell death following ischemic stroke include the failure of energy metabolism, glutamate excitotoxicity, free radical stress and inflammation among others. Most of the potential therapeutic interventions tried to target one or more of these deleterious events without a single clinical success. Recent evidences indicated that each of these mechanisms may have some neurorestorative role at some point of time during the evolution of cerebral I/R injury [2, 3]. Thus temporal considerations are important as terminating the therapy in time may be equally important as its well-timed initiation to extract maximum clinical advantage. Further, evaluation of the efficacy of the therapy will remain a serious challenge in absence of any standard diagnostic protocol to demarcate and measure the ischemic penumbra, core and the normal tissue as they usually remain scattered and highly heterogeneous [44]. Animal models of stroke are more uniform and can be controlled precisely to represent specific types of human stroke. MCA, being one of the most common sites of human large artery stroke, makes MCAO, a clinically relevant and the most widely accepted rodent model of cerebral ischemia. The use of

intraluminal filament MCAO model [22] made the surgery less invasive with easy manipulation to produce both ischemia and reperfusion injury in an extracranial manner. Hence, the first part of the study was concerned about establishing and validating the rat MCAO model of cerebral I/R injury. The duration of occlusion was fixed at 2 h to obtain reproducible infarction with lesser intergroup variation [23, 35]. This 2 h MCAO model is characterized by maximum infarction and vasogenic edema during 24 h -48 h post reperfusion. Thus, to evaluate the proteome regulation due to ischemia and early and intermediate phase of reperfusion injury, three groups of rats with only 2 h of ischemia followed by two different lengths of reperfusion (4 h and 24 h) were included in the experimental design (Figure 1).

The final ischemic area as a result of occlusion of MCA is rather consistent in this model. But the salvageable brain tissue decreases continuously due to the expansion of injury from the core to the penumbral area during reperfusion making it difficult to select specific area of ipsilateral hemisphere for temporal profiling. We aimed to elucidate the evolution of I/R injury as a function of time by using quantitative proteomics strategy. Thus, the whole ipsilateral cerebral hemisphere (excluding the olfactory lobe and cerebellum) were selected in our temporal proteomics experiment and comparison was made between groups of normal and I/R-affected animals. Moreover, pooling the whole hemisphere from three different animals minimized the surgical and biological variations between individual subjects. Finally, the whole hemispheric target identification strategy guided the selection of perturbed candidates for spatio-temporal profiling by WB analysis with three biological replicates for each group (except sham, where n=1) to show the biological variation.

Unraveling the Temporal Evolution of Ischemic Pathophysiology by the Analysis of the iTRAQ Dataset

The final list of proteins (Table 3) was functionally analyzed to interpret the molecular events relevant to the pathophysiology of cerebral ischemia in a chronological way.

Alteration of Energy Metabolism and Glutamate Excitotoxicity – Neuron-Astrocyte Cross-talk

Focal ischemia is associated with an acute release of a massive amount of glutamate by the glutaminergic synapses that represent > 85% of the cortical synapses [45]. In neurons, Glud1 plays essential role in generating releasable glutamate stored in the synaptic vesicles. Increased *in vivo* release of glutamate has been observed after neuronal depolarization in transgenic mice overexpressing Glud1 [46]. Thus, significant upregulation of Glud1 following 2 h of MCAO indicated the excitotoxic release of glutamate in the ischemic brain by the depolarized neurons. The excess glutamate in the synaptic cleft is quickly taken up by the specific high-affinity excitatory amino acid transporters (mainly Slc1a3 and Slc1a2) under physiological conditions to prevent overstimulation of the neuronal glutamate receptors (Figure 8). Their predominant astrocytic localization justifies the significant upregulation(Table 3, Figure 6B) following 4 h of reperfusion after 2 h of MCAO as seen with cultured astrocytes upon glutamate exposure [47]. Additionally, the upregulation of ubiquitous Glud1 in astrocytes would complement this glutamate uptake by using the neurotransmitter as an energy substrate to replenish α-keto glutarate along with ammonium ion to sustain the TCA cycle. Immunoreactivity of Glud1 in the astrocytic processes surrounding the glutaminergic nerve endings had been observed providing indirect evidence to the above event [48]. Depletion of negative regulator, GTP or increase in positive regulator, ADP under ischemic conditions will promote the ammoniagenesis through the forward reaction by Glud1, having a pH-stabilizing effect on the lactic acidosis, the well known early event in the pathophysiological cascade of stroke. Increased catabolism of glutamate by

stabilization of Glud1 mRNA in rat kidney following metabolic acidosis [49] or its upregulation both at the mRNA and protein level in the rat brain neuroblastoma cell line under conditions of simulated hypoxia or ischemia [21] were suggestive of the above phenomenon.

It is conceivable that acute shortage of blood-borne glucose and oxygen following 2 h of ischemia will shift the brain energy metabolism from aerobic to anaerobic mode with active participation of astrocytes due to their ability to use stored glycogen. The brain-specific isoform of glycogen phosphorylase, Pygb with predominant astrocytic localization will supplement glucose-6-phosphate from glycogen and can further save one mole of ATP thus making it an attractive substrate under ischemic conditions [50]. Predictably, glycogenolysis mediated rapid decrease in brain glycogen level has been observed in a model of *in vitro* ischemia using guinea pig hippocampal slice culture [51]. Hence, a concomitant upregulation of Pygb and several glycolytic enzymes (Tpi1, Pgam1, Pgk1 etc.) after 2 h of MCAO (Figure 6A) indicated increased mobilization of astrocytic glycogen in an ischemic brain for the first time to the best of our knowledge. The relative decrease of all regulated glycolytic enzymes along with Pygb after 4 h of reperfusion compared to 2 h of ischemia (Table 3) were attributed to the blood supply induced restoration of glucose-driven aerobic metabolism in most parts of the ischemic territory causing compensatory decrease on glycogen dependency.

Therefore, detailed understanding of these astrocyte-mediated survival responses could provide important insights about the evolution of cerebral I/R injury and metabolically targeted stroke therapeutics.

Neuroinflammation and Failure of Iron Homeostasis

Our study provided evidence that the breakdown of the BBB starts in parallel with the early events like failure of the energy metabolism or glutamate excitotoxicity and precedes serious

tissue damage [41]. This hyper-acute opening of the BBB may cause a leakage of the brain-specific proteins to the circulation that can be potential serum-specific prognostic marker for predicting the therapeutic outcome or progression of the disease. Reportage of many brain specific proteins from our dataset as potential serum biomarker for stroke (Gfap, Uchl1, S100B) [52, 53] is consistent with the above hypothesis. Conversely, tissue-based proteomics profiling may be an alternative way for stroke-biomarker discovery due to the presence of the permeable BBB. In addition, concentration of the extravasated acute phase proteins in the circulation may be reduced as seen for Tf in stroke patients [15] or synthesis by the target organ (e.g. liver) may be increased as a part of a compensatory response to provide surrogate markers for stroke. Nonetheless, some of the novel candidates (Pregnancy-zone protein or Isoform 1 of Murinoglobulin-1 precursor) from this group (Table 3) may be useful for prospective validation study to improve the sensitivity or specificity of the commonly used biomarkers to predict long term mortality after acute ischemic stroke.

Peaking of Hbb after 2 hr of ischemic injury (Table 3) was contributed by the serum-free hemoglobin (Hb) originated from the intravascular hemolysis as intact red blood cells (RBC) (diameter: 5 µm) cannot extravasate into brain parenchyma at an early stage [54]. In turn, it reconfirms the leakage of BBB immediately after ischemic injury. Recently free Hb in serum has been found to be associated with atherosclerosis and stroke and proposed as a potential biomarker for ischemic stroke [55]. The reperfusion probably restored the normalcy partly by decreasing the intravascular hemolysis although the leakage of serum-free Hb increased due to progressive opening of BBB. So, Hbb was continued to be detected till 24 h post reperfusion with a decreasing magnitude.

Unilateral increase of multiple acute phase proteins (e.g. Tf, Cp, Hpx) (Figure 6C) in the affected hemisphere that are involved in mobilization of iron to and from the brain cells (transporting iron as well as during transit from the circulation to the storage form to the cellular enzymes), indicated disruption of iron homeostasis during the course of cerebral I/R injury. Recently, Involvement of clathrin has been suggested in glutamate excitotoxicity induced endocytosis following brief episodes of ischemia in the viable neurons [56]. Our study showed increased expression of clathrin in the ischemic hemisphere during excitotoxicity after prolonged I/R injury, indicating the presence of viable and endocytic neurons that can also participate in the uptake of the apo- or holo-Tf following their leakage into the extracellular space [15]. Further, the uniform level of Tf mRNA (Figure 5B) precludes significant over-expression and de novo synthesis of this protein unlike albumin [42] in the I/R-insulted brain. This not only confirmed the circulatory origin of Tf but also indicated the failure of brain's endogenous defense mechanisms in response to the overwhelming oxidative stress.

Taken together, hyperacute yet progressive opening of BBB with a protein-specific dynamics will have clinical implications not only because of the efficacy of the sole approved medication for stroke (rt-PA) in the similar timeframe (i.e. maximum 4.5 h of window of opportunity [1]) but also the delivery and the pharmacokinetics of prospective drugs in analogous rodent models are critically dependent on plasma protein binding and permeability of BBB.

Transferrin, a Marker of Neuroinflammation

The central role of Tf in neuroinflammation and deregulated iron homeostasis had prompted us to check its spatio-temporal distribution in the affected area of the ipsilateral hemisphere to find the correlation between the Tf level and BBB failure. Our result proved that the BBB opening is not an all-or-none phenomenon; rather it is a gradual and progressive event. The overlap in the

pattern of core expansion and Tf presence can potentially make it a marker for BBB breakdown in similar experimental setting to understand neuro-inflammation.

The other selected candidate, Gfap is an astrocyte-specific protein that has been suggested as a sensitive serum-specific marker of brain damage in patients with smaller lacunar lesions or minor strokes [57] or traumatic brain injury [58]. Down regulation of Gfap in part II (core of injury) at 4 h post reperfusion is due to astrocytic damage during early reperfusion, whereas increasing trend after 24 h of I/R injury is indicative of reactive gliosis in response to neuroinflammation to promote endogenous repair. So, our study provided unique opportunity to compare the regional and temporal heterogeneity of two potential biomarkers in the ischemic hemisphere having extra-cranial and brain-specific origin. Increase in the ratio of Tf/Gfap compared to normal brain in the core during early reperfusion before appearance of detectable tissue damage could act as a pathological marker for irreversible brain damage in the post-stroke scenario.

Presence of Stroke Induced Plasticity

Although opening of the BBB caused severe neuro-inflammation, early fall in the level of several structural proteins (Plec1, Dync1h1, Spnb3) indicated irreversible activation of intracellular proteases and TTC staining showed presence of massive infarct by 24 h of reperfusion, we were also able to detect survival response in the form of higher expression of some growth promoting proteins. Increased expression of cell-specific makers (e.g. glial Gfap, neuronal Gap43, etc) indicated activation of specific components of neurovascular unit (astrocyte and neuron respectively) that constitute the survival response of the I/R injured brain by remodeling and re-establishing new connections. Upregulation of Gfap and Vim at 24 h post reperfusion (Table 3) were hallmarks of reactive gliosis in the post-ischemic brain. These proteins participate in the formation of the intermediate filament network in astrocytes that is a

part of the cytoskeleton. The stress induced activation of astrocytes may contribute in the repair or regeneration of the BBB, neurovascular unit, and the neuron [59]. Gap43 is a key indicator of synaptic plasticity, neuronal development and regeneration [60]. In addition, many proteins related to cell structure, proliferation, and differentiation (e.g. Myh10, Nefl, Tpm3) were significantly perturbed by the ischemic insult and over-expressed following 24 h of post-reperfusion. Thus our study corroborate with others who showed the presence of viable neurons following 24 h or at later time points (48 h or 52 h) [44] using imaging techniques. All these proteins may be accounted for the spontaneous recovery in neurological impairment, observed at 24 h post-reperfusion.

Identification of Novel Candidates in Stroke Pathology

A host of proteins never reported in context of stroke were also regulated during the course of I/R injury (Table 3, Figure 6D). The downregulated proteins like, Caskin1 or Isoform L of Band 4.1-like protein 1(Epb4.1l1) had direct interaction with a synaptic scaffolding protein, CASK of Membrane-associated guanylate kinase family. Similarly, both Caskin1 and Shank3 were located in the post synaptic density having multidomain scaffolds. Intriguingly, their domain composition was found to be similar (presence of SH3 domain and SAM domains) amid differences in precise number, type, arrangement and sequence of certain domains. This probably reflects similar scaffolding function and explains the concomitant down regulation in the current model [61]. Thus, parallel downregulation of all these proteins at 24 h post I/R injury is closely associated and may indicate general decline in normal synaptic functions. Recently, shank proteins, which organize the glutamate receptors at excitatory synapses, were altered in AD affected brains due to abnormal activity of ubiquitin-proteosome system (UPS) with Shank3 showing significant down-regulation [62]. Similar mechanisms can also be implicated in our model as two proteins related to UPS were upregulated (Uchl1 and Ube1x) indicating its abnormal

regulation. Uchl1, a deubiquitinating enzyme present throughout the brain, has also been proposed as a potential biomarker for I/R injury using a 2 h MCAO model [53]. Mtap6 or STOP (stable tubule only polypeptides) is a class of microtubule associated calmodulin-binding and calmodulin-regulated protein, responsible for cold stabilization of microtubule in both neuronal and non-neuronal cells. Recent studies with Mtap6-/- null mice have indicated that suppression of Mtap6 can cause synaptic defects associated with severe behavioral disorders like schizophrenia [63]. Thus, significant down-regulation of Mtap6 at 4 h and 24 h post reperfusion could be related to the compromised state of synaptic plasticity.

It is fascinating that many of the novel regulated synaptic proteins (Mtap6, Apba1, Shank3, and Ctnnd2) have been implicated in chronic neurodegenerative or psychiatric disorders. Hence, further studies are necessary to determine their participation in the pathology of stroke-induced motor, cognitive or neuropsychiatric disorders like post-stroke or vascular dementia [64] and stroke-induced depression, anxiety or psychosis, conditions where ischemic stroke acts as a predisposing factor [65].

CONCLUDING REMARKS

By applying iTRAQ coupled with 2D-LC-MS/MS, we capture for the first time the global-temporal protein expression profile of the affected hemisphere in a validated *in vivo* model of transient focal cerebral ischemia. This regulated list will offer a reference dataset for the future studies with analogous rodent or primate models, especially in absence of a comparable dataset from the human ischemic brain samples. It revealed brain's response to ischemia and reperfusion injury simultaneously to better understand the temporal dynamics of the key facets of stroke pathophysiology (e.g. alterations of energy metabolism, glutamate excitotoxicity, neuroinflammation etc.) unfolding concurrently in an interconnected manner. Demonstration of

several proteins (Caskin1, Shank3, Kpnb1, Uchl1, Mtap6, Epb4.1l1, Apba1, Ube1x) novel in context of stroke pathology as regulated one, proved the utility of this discovery approach. In addition, validation of Caskin-1 confirmed its technical reliability as do other validated candidates from the dataset. Remarkably, this was achieved with a single experimental paradigm without involving any sub-cellular fractionation or using specialized sample processing techniques or targeting particular brain regions. The sheer number of proteins with confident quantitative information makes the iTRAQ-based quantitative proteomics as the preferred approach for therapeutic target discovery [21]. Hence, the regulated proteins can be exploited for their validity as serum-specific prognostic biomarker or pharmacodynamic biomarker for checking the consequence of drug-target interaction or for reporting the efficacy of the prospective therapeutic candidates on progression of the I/R injury [1]. Additionally, the individual proteins can further be explored through functional studies in animal or simpler cell-line models.

The detection of system-level emergent properties, like identification of metabolic cross-talk in between neurons and astrocytes and breakdown of BBB in the ischemic brain is only amenable by an *in vivo* profiling approach. The active involvement of astrocytes as a savior of neurons during the acute phase of I/R injury substantiates the changing priorities of stroke research from neuron-specific to cerebro-specific approaches that includes the whole neurovascular unit [66]. BBB damage, despite being reported as a hyperacute event, evolved gradually along with iron mediated neurotoxicity, providing a wider therapeutic window. The differential spatio-temporal response of Tf and Gfap between areas of ispilateral brain proved that the approach can be extended for other regulated proteins to generate a pathological fingerprint of specific substructures of the brain to propose event-specific spatio-temporal markers. In addition, late recovery or up-regulation of expression of several structural (myosin-10, plectin 3) and

regenerative proteins (Gfap, Vim, Gap43 etc.) indicated the presence of putative pleiotropic mechanisms with ample opportunity to promote brain repair by favorably modulating these sub-acute or chronic events.

The phasic response of multiple players during the first 24 h of cerebral I/R injury argues against the conventional approach of sustained and unilateral modulation of certain targets. In turn, it supports a combination therapy involving multiple targets and addresses the need for carefully designing the therapeutic strategy during future clinical trials depending on the temporal profile of the respective targets. Concluding, we provide a new strategy in the area of stroke-neuroproteomics for unraveling the hitherto novel molecular mechanisms of cerebral I/R injury.

Acknowledgement

The authors thank Lokesh Bhatt, Prashant G J, Anookh Mohanan, Salil Kumar Bose, Jung Eun Park, Xin Li, Anindya Basu, Guo Tiannan and Yi Zhu for the experimental assistance and critical reading of the manuscript. The work is supported by grants from the Agency for Science, Technology and Research (BMRC: 08/1/22/19/575) and the Ministry of Education (ARC: T206B3211) of Singapore.

Supporting Information Available

Supplemental Table 1, Primer sequences of the genes selected for RT-PCR from the regulated list of proteins following iTRAQ experiment. Supplemental Table 2, Summary of the physiological parameters of the four participating Groups in the iTRAQ experiment. Supplemental Table 3(A), Complete information of the full list of the qualified proteins (Unused prot sore ≥ 2, p-value < 0.05 for at least one ratio) obtained from the bias and background corrected iTRAQ dataset. Supplemental Table 3(B), Complete information of the proteins

included in Table 3 (Result Section) based on their identification information only due to their close association with the regulated proteins. Supplemental Table 4, Pathway Analysis of the regulated and validated proteins from the iTRAQ dataset by PANTHER 7.0.

Supplemental Figure 1, Changes in physiological variables of Sprague Dawley rat in MCAO model of cerebral I/R injury and sham group. Supplemental Figure 2, Evolution of cumulative neurological score during the course of cerebral I/R injury. Supplemental Figure 3, Determination of ratio-specific technical variation using 1166 commonly quantified proteins (unused prot score >2.0) from the three technical replicates.

Supplemental Data A, Calculation of FDR for each technical replicate and combined dataset.

Supplemental Data B, Geometric Mean and Standard Deviation in log space for iTRAQ ratios from three technical replicates. Supplemental Data C, Combined Protein summary from three technical replicates. Supplemental Data D, Combined Peptide summary from three technical replicates. This material is available free of charge via the Internet at http://pubs.acs.org.

REFERENCES

1. Zaleska, M. M.; Mercado, M. L. T.; Chavez, J.; Feuerstein, G. Z.; Pangalos, M. N.; Wood, A., The development of stroke therapeutics: Promising mechanisms and translational challenges. *Neuropharmacology* **2009,** 56, 329-341.

2. Ikonomidou C Fau - Turski, L.; Turski, L.; Hoyte L Fau - Barber, P. A.; Barber Pa Fau - Buchan, A. M.; Buchan Am Fau - Hill, M. D.; Hill, M. D., Why did NMDA receptor antagonists fail clinical trials for stroke and traumatic brain injury? The rise and fall of NMDA antagonists for ischemic stroke. *Lancet Neurology* **2002,** 1, (6), 383-386.

3. Lo, E. H., A new penumbra: Transitioning from injury into repair after stroke. *Nature Medicine* **2008,** 14, (5), 497-500.

4. Moskowitz, M. A.; Lo, E. H.; Iadecola, C., The science of stroke: Mechanisms in search of treatments. *Neuron* **2010,** 67, (2), 181-198.

5. Choudhary, J.; Grant, S. G. N., Proteomics in postgenomic neuroscience: The end of the beginning. *Nature Neuroscience* **2004,** 7, (5), 440-445.

6. Luo, Y.; Yin, W.; Signore, A. P.; Zhang, F.; Hong, Z.; Wang, S.; Graham, S. H.; Chen, J., Neuroprotection against focal ischemic brain injury by the peroxisome proliferator-activated receptor-γ agonist rosiglitazone. *Journal of Neurochemistry* **2006,** 97, (2), 435-448.

7. Sung, J. H.; Cho, E. H.; Kim, M. O.; Koh, P. O., Identification of proteins differentially expressed by melatonin treatment in cerebral ischemic injury - A proteomics approach. *Journal of Pineal Research* **2009,** 46, (3), 300-306.

8. Zhang, Z.; Wu, R.; Li, P.; Liu, F.; Zhang, W.; Zhang, P.; Wang, Y., Baicalin administration is effective in positive regulation of twenty-four ischemia/reperfusion-related proteins identified by a proteomic study. *Neurochemistry International* **2009,** 54, (8), 488-496.

9. Dhodda, V. K.; Sailor, K. A.; Bowen, K. K.; Vemuganti, R., Putative endogenous mediators of preconditioning-induced ischemic tolerance in rat brain identified by genomic and proteomic analysis. *J Neurochem* **2004,** 89, (1), 73-89.

10. Cid, C.; Garcia-Bonilla, L.; Camafeita, E.; Burda, J.; Salinas, M.; Alcazar, A., Proteomic characterization of protein phosphatase 1 complexes in ischemia-reperfusion and ischemic tolerance. *Proteomics* **2007,** 7, (17), 3207-3218.

11. Chen, A.; Liao, W. P.; Lu, Q.; Wong, W. S. F.; Wong, P. T. H., Upregulation of dihydropyrimidinase-related protein 2, spectrin α II chain, heat shock cognate protein 70 pseudogene 1 and tropomodulin 2 after focal cerebral ischemia in rats-A proteomics approach. *Neurochemistry International* **2007,** 50, (7-8), 1078-1086.

12. Carmichael, S. T., Rodent models of focal stroke: Size, mechanism, and purpose. *NeuroRx* **2005,** 2, (3), 396-409.

13. Fisher, M.; Feuerstein, G.; Howells, D. W.; Hurn, P. D.; Kent, T. A.; Savitz, S. I.; Lo, E. H., Update of the stroke therapy academic industry roundtable preclinical recommendations. *Stroke* **2009,** 40, (6), 2244-2250.

14. Wang, X.; Lo, E. H., Triggers and Mediators of Hemorrhagic Transformation in Cerebral Ischemia. *Molecular Neurobiology* **2003,** 28, (3), 229-244.

15. Altamura, C.; Squitti, R.; Pasqualetti, P.; Gaudino, C.; Palazzo, P.; Tibuzzi, F.; Lupoi, D.; Cortesi, M.; Rossini, P. M.; Vernieri, F., Ceruloplasmin/Transferrin system is related to clinical status in acute stroke. *Stroke* **2009,** 40, (4), 1282-1288.

16. Domínguez, C.; Delgado, P.; Vilches, A.; Martín-Gallán, P.; Ribó, M.; Santamarina, E.; Molina, C.; Corbeto, N.; Rodríguez-Sureda, V.; Rosell, A.; Alvarez-Sabín, J.; Montaner, J.,

Oxidative stress after thrombolysis-induced reperfusion in human stroke. *Stroke* **2010,** 41, (4), 653-660.

17. Koh, P. O., Proteomic analysis of focal cerebral ischemic injury in male rats. *Journal of Veterinary Medical Science* **2010,** 72, (2), 181-185.

18. Washburn, M. P.; Wolters, D.; Yates, J. R., Large-scale analysis of the yeast proteome by multidimensional protein identification technology. *Nature Biotechnology* **2001,** 19, (3), 242-247.

19. Gygi, S. P.; Rist, B.; Gerber, S. A.; Turecek, F.; Gelb, M. H.; Aebersold, R., Quantitative analysis of complex protein mixtures using isotope-coded affinity tags. *Nature Biotechnology* **1999,** 17, (10), 994-999.

20. Park, J. E.; Tan, H. S.; Datta, A.; Lai, R. C.; Zhang, H.; Meng, W.; Lim, S. K.; Sze, S. K., Hypoxic tumor cell modulates its microenvironment to enhance angiogenic and metastatic potential by secretion of proteins and exosomes. *Molecular and Cellular Proteomics* **2010,** 9, (6), 1085-1099.

21. Datta, A.; Park, J. E.; Li, X.; Zhang, H.; Ho, Z. S.; Heese, K.; Lim, S. K.; Tam, J. P.; Sze, S. K., Phenotyping of an in vitro model of ischemic penumbra by iTRAQ-based shotgun quantitative proteomics. *Journal of Proteome Research* **2010,** 9, (1), 472-484.

22. Longa, E. Z.; Weinstein, P. R.; Carlson, S.; Cummins, R., Reversible middle cerebral artery occlusion without craniectomy in rats. *Stroke* **1989,** 20, (1), 84-91.

23. Belayev, L.; Busto, R.; Zhao, W.; Fernandez, G.; Ginsberg, M. D., Middle cerebral artery occlusion in the mouse by intraluminal suture coated with poly-L-lysine: Neurological and histological validation. *Brain Research* **1999,** 833, (2), 181-190.

24. Zausinger, S.; Hungerhuber, E.; Baethmann, A.; Reulen, H. J.; Schmid-Elsaesser, R., Neurological impairment in rats after transient middle cerebral artery occlusion: a comparative study under various treatment paradigms. *Brain Research* **2000,** 863, (1-2), 94-105.

25. Joshi, C. N.; Jain, S. K.; Murthy, P. S. R., An optimized triphenyltetrazolium chloride method for identification of cerebral infarcts. *Brain Research Protocols* **2004,** 13, (1), 11-17.

26. Belayev, L.; Alonso, O. F.; Busto, R.; Zhao, W.; Ginsberg, M. D., Middle cerebral artery occlusion in the rat by intraluminal suture: Neurological and pathological evaluation of an improved model. *Stroke* **1996,** 27, (9), 1616-1623.

27. Liao, L.; McClatchy, D. B.; Yates, J. R., Shotgun proteomics in neuroscience. *Neuron* **2009,** 63, (1), 12-26.

28. Chong, P. K.; Gan, C. S.; Pham, T. K.; Wright, P. C., Isobaric tags for relative and absolute quantitation (iTRAQ) reproducibility: Implication of multiple injections. *Journal of Proteome Research* **2006,** 5, (5), 1232-1240.

29. Traystman, R. J., Effect of anesthesia in stroke models. *Neuromethods* **2010,** 47, 121-138.

30. Kersey, P. J.; Duarte, J.; Williams, A.; Karavidopoulou, Y.; Birney, E.; Apweiler, R., The International Protein Index: an integrated database for proteomics experiments. *Proteomics* **2004,** 4, (7), 1985-8.

31. Elias, J. E.; Gygi, S. P., Target-decoy search strategy for increased confidence in large-scale protein identifications by mass spectrometry. *Nature Methods* **2007,** 4, (3), 207-214.

32. Thomas, P. D.; Campbell, M. J.; Kejariwal, A.; Mi, H.; Karlak, B.; Daverman, R.; Diemer, K.; Muruganujan, A.; Narechania, A., PANTHER: A library of protein families and subfamilies indexed by function. *Genome Research* **2003,** 13, (9), 2129-2141.

33. del Zoppo, G. J., Microvascular changes during cerebral ischemia and reperfusion. *Cerebrovascular and brain metabolism reviews* **1994,** 6, (1), 47-96.

34. Dittmar, M.; Spruss, T.; Schuierer, G.; Horn, M., External carotid artery territory ischemia impairs outcome in the endovascular filament model of middle cerebral artery occlusion in rats. *Stroke* **2003,** 34, (9), 2252-2257.

35. Li, F.; Omae, T.; Fisher, M., Spontaneous hyperthermia and its mechanism in the intraluminal suture middle cerebral artery occlusion model of rats. *Stroke* **1999,** 30, (11), 2464-2471.

36. Schmid-Elsaesser, R.; Zausinger, S.; Hungerhuber, E.; Baethmann, A.; Reulen, H. J., A critical reevaluation of the intraluminal thread model of focal cerebral ischemia: Evidence of inadvertent premature reperfusion and subarachnoid hemorrhage in rats by laser-Doppler flowmetry. *Stroke* **1998,** 29, (10), 2162-2170.

37. Zhang, X.; Deguchi, K.; Yamashita, T.; Ohta, Y.; Shang, J.; Tian, F.; Liu, N.; Panin, V. L.; Ikeda, Y.; Matsuura, T.; Abe, K., Temporal and spatial differences of multiple protein expression in the ischemic penumbra after transient MCAO in rats. *Brain Research* **2010,** 1343, (C), 143-152.

38. Weinstein, P. R.; Hong, S.; Sharp, F. R., Molecular identification of the ischemic penumbra. *Stroke* **2004,** 35, (11 SUPPL. 1), 2666-2670.

39. Chee, S. G.; Poh, K. C.; Trong, K. P.; Wright, P. C., Technical, experimental, and biological variations in isobaric tags for relative and absolute quantitation (iTRAQ). *Journal of Proteome Research* **2007,** 6, (2), 821-827.

40. Arranz, A. M.; Gottlieb, M.; Perez-Cerda, F.; Matute, C., Increased expression of glutamate transporters in subcortical white matter after transient focal cerebral ischemia. *Neurobiology of Disease* **2010,** 37, (1), 156-165.

41. Ishii, T.; Asai, T.; Urakami, T.; Oku, N., Accumulation of macromolecules in brain parenchyma in acute phase of cerebral infarction/reperfusion. *Brain Research* **2010,** 1321, (C), 164-168.

42. Prajapati, K. D.; Sharma, S. S.; Roy, N., Upregulation of albumin expression in focal ischemic rat brain. *Brain Research* **2010,** 1327, (C), 118-124.

43. Brilli, E.; Scali, M.; Casarosa, S.; Kohler, M.; Bozzi, Y., Seizures increase importin-beta1 expression in NG2+ cells in the rat hippocampus. *J Neurosci Res* **2009,** 87, (3), 636-43.

44. Wardlaw, J. M., Neuroimaging in acute ischaemic stroke: Insights into unanswered questions of pathophysiology. *Journal of Internal Medicine* **2010,** 267, (2), 172-190.

45. Magistretti, P. J., Role of glutamate in neuron-glia metabolic coupling. *American Journal of Clinical Nutrition* **2009,** 90, (3), 875S-880S.

46. Bao, X.; Pal, R.; Hascup, K. N.; Wang, Y.; Wang, W. T.; Xu, W.; Hui, D.; Agbas, A.; Wang, X.; Michaelis, M. L.; Choi, I. Y.; Belousov, A. B.; Gerhardt, G. A.; Michaelis, E. K., Transgenic expression of Glud1 (glutamate dehydrogenase 1) in neurons: In vivo model of enhanced glutamate release, altered synaptic plasticity, and selective neuronal vulnerability. *Journal of Neuroscience* **2009,** 29, (44), 13929-13944.

47. Duan, S.; Anderson, C. M.; Stein, B. A.; Swanson, R. A., Glutamate induces rapid upregulation of astrocyte glutamate transport and cell-surface expression of GLAST. *Journal of Neuroscience* **1999,** 19, (23), 10193-10200.

48. Aoki, C.; Milner, T. A.; Berger, S. B.; Sheu, K. F. R.; Blass, J. P.; Pickel, V. M., Glial glutamate dehydrogenase: ultrastructural localization and regional distribution in relation to the mitochondrial enzyme, cytochrome oxidase. *Journal of Neuroscience Research* **1987,** 18, (2), 305-318.

49. Schroeder, J. M.; Liu, W.; Curthoys, N. P., pH-responsive stabilization of glutamate dehydrogenase mRNA in LLC-PK_1-F^+ cells. *American Journal of Physiology - Renal Physiology* **2003,** 285, F258-F265.

50. Brown, A. M.; Sickmann, H. M.; Fosgerau, K.; Lund, T. M.; Schousboe, A.; Waagepetersen, H. S.; Ransom, B. R., Astrocyte glycogen metabolism is required for neural activity during aglycemia or intense stimulation in mouse white matter. *Journal of Neuroscience Research* **2005,** 79, (1-2), 74-80.

51. Lipton, P., Regulation of glycogen in the dentate gyrus of the in vitro guinea pig hippocampus; effect of combined deprivation of glucose and oxygen. *Journal of Neuroscience Methods* **1989,** 28, (1-2), 147-154.

52. Whiteley, W.; Chong, W. L.; Sengupta, A.; Sandercock, P., Blood markers for the prognosis of ischemic stroke: A systematic review. *Stroke* **2009,** 40, (5), e380-e389.

53. Liu, M. C.; Akinyi, L.; Scharf, D.; Mo, J.; Larner, S. F.; Muller, U.; Oli, M. W.; Zheng, W.; Kobeissy, F.; Papa, L.; Lu, X. C.; Dave, J. R.; Tortella, F. C.; Hayes, R. L.; Wang, K. K., Ubiquitin C-terminal hydrolase-L1 as a biomarker for ischemic and traumatic brain injury in rats. *Eur J Neurosci* **2010,** 31, (4), 722-32.

54. Nagaraja, T. N.; Keenan, K. A.; Fenstermacher, J. D.; Knight, R. A., Acute leakage patterns of fluorescent plasma flow markers after transient focal cerebral ischemia suggest large openings in blood-brain barrier. *Microcirculation* **2008,** 15, (1), 1-14.

55. Huang, P.; Lo, L. H.; Chen, Y. C.; Lin, R. T.; Shiea, J.; Liu, C. K., Serum free hemoglobin as a novel potential biomarker for acute ischemic stroke. *Journal of Neurology* **2009,** 256, (4), 625-631.

56. Yoshimi, K.; Iwata, N.; Takeda, M.; Nakamura, Y.; Nishimura, T., Ischaemia-induced change in clathrin preceding delayed neuronal death. *NeuroReport* **1995,** 6, (3), 453-456.

57. Herrmann, M.; Vos, P.; Wunderlich, M. T.; De Bruijn, C. H. M. M.; Lamers, K. J. B., Release of glial tissue-specific proteins after acute stroke: A comparative analysis of serum concentrations of protein S-100B and glial fibrillary acidic protein. *Stroke* **2000,** 31, (11), 2670-2677.

58. Honda, M.; Tsuruta, R.; Kaneko, T.; Kasaoka, S.; Yagi, T.; Todani, M.; Fujita, M.; Izumi, T.; Maekawa, T., Serum glial fibrillary acidic protein is a highly specific biomarker for traumatic brain injury in humans compared with S-100B and neuron-specific enolase. *Journal of Trauma - Injury, Infection and Critical Care* **2010,** 69, (1), 104-109.

59. Pekny, M.; Nilsson, M., Astrocyte activation and reactive gliosis. *GLIA* **2005,** 50, (4), 427-434.

60. Yamada, K.; Goto, S.; Oyama, T.; Inoue, N.; Nagahiro, S.; Ushio, Y., In vivo induction of the growth associated protein GAP43/B-50 in rat astrocytes following transient middle cerebral artery occlusion. *Acta Neuropathologica* **1994,** 88, (6), 553-557.

61. Tabuchi, K.; Biederer, T.; Butz, S.; Südhof, T. C., CASK Participates in Alternative Tripartite Complexes in which Mint 1 Competes for Binding with Caskin 1, a Novel CASK-Binding Protein. *Journal of Neuroscience* **2002,** 22, (11), 4264-4273.

62. Gong, Y.; Lippa, C. F.; Zhu, J.; Lin, Q.; Rosso, A. L., Disruption of glutamate receptors at Shank-postsynaptic platform in Alzheimer's disease. *Brain Research* **2009,** 1292, (C), 191-198.

63. Bosc, C.; Andrieux, A.; Job, D., STOP Proteins. *Biochemistry* **2003,** 42, (42), 12125-12132.

64. Pendlebury, S. T., Stroke-related dementia: Rates, risk factors and implications for future research. *Maturitas* **2009,** 64, (3), 165-171.

65. Chemerinski, E.; Levine, S. R., Neuropsychiatric disorders following vascular brain injury. *Mount Sinai Journal of Medicine* **2006,** 73, (7), 1006-1014.

66. Lo, E. H.; Moskowitz, M. A.; Jacobs, T. P., Exciting, radical, suicidal: How brain cells die after stroke. *Stroke* **2005,** 36, (2), 189-192.

Figure legends

Figure 1. Schematic illustration of experimental design classified into iTRAQ based quantitative proteomics, data validation by complementary techniques and subsequent spatio-temporal profiling of selected candidates.

Figure 2. TTC staining of representative coronal sections from each group with a corresponding schematic diagram and respective anterio-posterior position to bregma (0 mm). Infarct area was maximum at the level of bregma (%HIA is 74% at 0.8 mm posterior to bregma) after 24 h of I/R injury. Small infarction was seen at around 1.2 mm anterior to bregma in 2+0 and 2+4 group. No ischemic lesion was observed in the sham group.

Figure 3. Molecular validation of the rat MCAO model of I/R injury by WB analysis. Pooled lysate from each group were probed with monoclonal antibodies against Hsp70 and Hif1a along with actin as loading control. Hsp70 expression was high till 24 h of I/R injury, whereas expression of Hif1a peaked at 4 h post reperfusion.

Figure 4. Validation of selected proteins by WB analysis. Cytoskeletal proteins (Gfap, Vim, Vcl) and Tf peaked 24 h after I/R injury. Slc1a3 expression was maximum at 4 h post reperfusion while Caskin1 showed a gradual decline till 24 h post reperfusion. Actn1 was used as loading control.

Figure 5. Representative images of the temporal regulation of the selected genes from the iTRAQ dataset. (A) Genes related to cerebral plasticity. Nefl showed a biphasic response with increase at 2+0 and 2+24 group. Tpm3 was upregulated in all three groups except sham, whereas Gfap exhibited a late upregulation after 24 h of reperfusion. (B) Genes of circulatory proteins.

C3 showed an increasing trend at 4 h and 24 h of I/R injury, whereas Tf did not show any change. (C) Regulation of novel candidate, Caskin1 showed down-regulation at 24 h post reperfusion.

Figure 6. Histograms showing relative temporal expression patterns of regulated proteins in the ischemic hemisphere during the course of cerebral I/R injury. Natural logarithm of iTRAQ ratios of the proteins with respect to sham group were plotted in the vertical axis. The gene symbols were plotted in the horizontal axis. (A) Proteins related to glycolysis and glycogen mobilization showed persistent upregulation. (B) Proteins taking part in glutamate excitotoxicity were mostly upregulated especially after 4 h of reperfusion except the neuronal subtype of glutamate transporter, Slc1al, which showed a downward trend. (C) Increasing trend of all circulatory proteins (except Hbb) signified gradual leakage of BBB causing progressive vasogenic edema (D) Synapse related proteins (Mtap6, Epb41l1, Caskin1, Shank3, Ctnnd2, Apba1) exhibited generalized downward trend implying compromised synaptic function.

Figure 7. Spatio-temporal profiling of validated candidates (Tf and Gfap) by WB analysis in the core and penumbra of the cerebral I/R injury. Actin was used as loading control. Each time point has three biological replicates except sham. Early opening of BBB in the core of injury (part II) as seen by the leakage of circulatory Tf at 4 h post-reperfusion. Gfap showed a reverse trend in the core at the same time signifying the astrocytic damage. Recovery of Gfap level in both parts after 24 h post I/R injury was indicative of the reactive gliosis, constituting a recovery response.

Figure 8. Schematic diagrams showing the interplay of glucose metabolism, glutamate excitotoxicity, neuroinflammation and deregulation of iron homeostasis in the neurovascular unit (neuron, black; astrocyte, blue; and vasculature, red border) of the ischemic brain. The gene symbols with red color were identified in our experiment, whereas the one with bold red had at least one of the quantification ratio with significant *p* value. Multiple cell-specific roles of

glutamate in the form of neurotransmitter, metabolic intermediate and signaling molecule are shown that acted as a connecting link between glutamate excitotoxicity and altered energy metabolism. Both Glul and Pygb have predominantly astrocytic localization. Astrocytic glutamate uptake through upregulated transporters is coupled with increased Na^+-driven glucose uptake stimulating glycolysis in astrocytes during early reperfusion. Pygb would complement anaerobic glycolysis under ischemic condition by utilizing stored glycogen in the astrocytes. In the vessel lumen, vascular dysfunction and reactive oxygen species (ROS) induced hemolysis would produce serum free hemoglobin (Hbb), heme and iron. Hemopexin (Hpx) and ceruloplasmin (Cp) - Tf system would act to keep free heme or iron within normal limits. Vascular dysfunction and free radical mediated leakage of BBB would cause accumulation of several circulatory proteins (Tf, Cp, Hpx, Hbb etc.) inside the brain with increased presence after 24 h of I/R injury. ETC is electron transport chain; Hk1 is hexokinase-1; Glc-6-P is glucose-6-phosphate; α-KG is α-keto glutarate; TCA is tricarboxylic acid.

Tables

Table 1. Summary of the group allocation for different experiments

Experiments	Purpose	Group of Animals			
		Sham	2+0 h	2+4 h	2+24 h
iTRAQ-2D-LC-MS/MS	Temporal profiling	3	3	3	3
WB	Validation	Same protein samples from iTRAQ experiment			
RT-PCR	Validation	2	2	2	2
WB	Spatio-temporal profiling	1	3	3	3

Table 2. Regulation of physiological variables during the course of cerebral I/R injury in Sprague Dawley rats [a]

Physiologic parameter	Condition	Groups			
		2 + 4 h		2 + 24 h	
% Decrease in Weight (g)	Surgery	3.67 ± 1.58		11.79 ± 2.54	
	Sham	1.49 ± 0.39		5.22 ± 1.76	
Temp (°C)		0 h	2 + 0 h	2 + 4 h	2 + 24 h
	Surgery	37.07 ± 0.39	38.77 ± 0.49	38.60 ± 0.42	38.16 ± 0.61
	Sham	37.23 ± 0.34	37.23 ± 0.61	37.50 ± 0.33	37.40 ± 0.57

[a] Data was presented as mean ± SD ($n \geq 6$, surgery; $n \geq 3$, sham). Body weight at 0 h post reperfusion and pre-operative rectal temperature (0 h) were used as respective controls for statistical test (one way ANOVA followed by Dunnett's Multiple Comparison Test). Significant increase in % loss of body weight and rectal temperature was observed following MCAO model of cerebral I/R injury in comparison to sham group of animals.

Table 3. Quantitative information of the significantly regulated proteins obtained from the bias and background corrected iTRAQ dataset showing a temporal pattern in the transient MCAO model of cerebral I/R injury [a]

N	Unused	%Cov (95)	Gene Symbol	Protein Name	Unique Peptides (95%)	Total Peptides (95%)	115:114 (2+0:sham)	116:114 (2+4:sham)	117:114 (2+24:sham)
				Energy Metabolism					
29	65.7	41.6	Pygb	brain glycogen phosphorylase	47	154	**3.08**	1.60	2.73
38	60.5	53.5	Atp5b	ATP synthase subunit beta, mitochondrial precursor	83	414	**3.63**	**3.37**	**3.53**
48	58.5	31.4	Hk1	Hexokinase-1 [d]	50	220	1.36	0.85	1.43
56	54.5	44.7	Atp5a1	ATP synthase subunit alpha, mitochondrial precursor	67	463	**2.42**	1.84	1.84
65	49.4	43.4	LOC688509	similar to Alpha-enolase	50	159	1.39	1.47	**1.72**
91	42.5	36.0	Ndufs1	NADH-ubiquinone oxidoreductase 75 kDa subunit, mitochondrial precursor [d]	31	87	1.46	1.21	1.71
119	38.0	49.2	Pgk1	Phosphoglycerate kinase 1	34	176	**2.56**	**2.36**	**2.56**
179	29.0	26.2	Pygm	Glycogen phosphorylase, muscle form [d]	23	50	1.33	0.97	1.11
216	25.6	60.2	Tpi1	Triosephosphate isomerase	20	50	**1.58**	1.37	**1.38**
333	18.8	28.5	Ndufs2	NADH dehydrogenase (Ubiquinone) Fe-S protein 2 [d]	10	22	1.27	1.33	1.15
357	17.7	37.0	Pgam1	Phosphoglycerate mutase 1	11	38	**2.56**	1.53	**1.84**
				Glutamate Excitotoxicity					
8	169.6	47.1	Cltc	Clathrin heavy chain	177	804	1.02	**1.94**	1.41
115	38.8	41.8	Glud1	Glutamate dehydrogenase 1, mitochondrial precursor	27	67	**4.25**	2.42	2.56
120	37.9	21.4	Slc1a2	Isoform Glt-1A of Excitatory amino acid transporter 2 [d]	39	289	1.10	1.82	1.28
152	31.8	36.5	Glul	Glutamine synthetase [d]	30	87	1.80	1.84	1.85

243	24.0	21.9	Slc1a3	Isoform GLAST-1 of Excitatory amino acid transporter 1 (EAAT1)	31	168	1.36	**1.64**	1.18
1387	4.0	6.5	Slc16a1	Monocarboxylate transporter 1 (MCT1) [d]	3	7	1.39	1.58	1.37
2070	2.0	4.8	Slc1a1	Excitatory amino acid transporter 3 [d]	2	3	0.86	0.79	0.91
				Neuro-inflammation and Iron Metabolism					
42	60.1	54.9	Alb	Serum albumin precursor	45	176	2.21	**18.20**	**24.89**
131	36.8	29.7	Tf	Isoform 1 of Serotransferrin precursor [c]	23	125	2.09	**6.25**	**9.55**
458	14.2	58.5	Hbb	Hemoglobin subunit beta-1	9	28	**3.47**	**2.96**	1.69
491	13.5	5.1	C3	Complement C3 precursor (Fragment) [c]	6	16	1.08	**7.59**	**7.18**
619	10.5	6.5	Cp	121 kDa protein	5	11	0.85	**2.54**	**4.13**
734	8.7	4.3	Pzp	Pregnancy-zone protein, 167 kDa protein	4	7	0.73	**7.31**	**6.49**
978	6.1	6.7	Hpx	Hemopexin precursor	3	4	1.63	**3.47**	**5.20**
1217	4.5	5.3	Fetub	Fetub protein	2	2	3.60	**7.59**	**14.59**
1242	4.3	5.7	Mug1	Isoform 1 of Murinoglobulin-1 precursor	7	14	1.04	**6.55**	**6.67**
2239	2.0	16.3	S100b	Protein S100-B [d]	3	37	1.45	2.05	2.10
				Cerebral Plasticity					
Synapse Related Proteins									
81	44.5	39.0	Mtap6	STOP protein	25	72	0.69	**0.45**	**0.51**
84	43.6	18.4	Epb4.1l1	Isoform L of Band 4.1-like protein 1	36	94	0.77	0.74	**0.55**
133	36.0	19.4	Caskin1	Caskin1[c]	22	44	0.61	**0.59**	**0.48**
155	31.4	13.1	Shank3	Isoform 1 of SH3 and multiple ankyrin repeat domains protein 3	15	36	0.81	0.94	**0.57**
269	22.4	11.4	Ctnnd2	similar to Catenin delta-2	11	31	0.82	**0.69**	**0.66**

974	6.1	5.7	Apba1	Amyloid beta A4 precursor protein-binding family A member 1	4	7	0.70	0.73	**0.59**
Structural Proteins									
1	396.7	63.2	Spna2	Spectrin alpha chain, brain	405	1957	**0.83**	1.15	1.43
2	287.7	36.7	Dync1h1	Dynein heavy chain, cytosolic	207	706	**0.64**	0.90	1.01
4	198.5	28.6	Plec1	Plectin 3	105	273	**0.56**	**0.96**	1.19
6	175.6	45.3	Spnb3	Spectrin beta chain, brain 2	142	524	**0.65**	0.88	0.94
7	173.8	42.0	Mtap1a	Microtubule-associated protein 1A	122	396	**0.94**	**0.63**	**0.94**
11	153.1	42.6	Myh10	Myosin-10	105	321	**0.57**	**0.77**	1.39
111	39.3	46.1	Nefl	Neurofilament light polypeptide [c]	39	127	**1.94**	1.04	**1.87**
141	33.4	47.7	Gfap	Isoform 1 of Glial fibrillary acidic protein [c]	27	92	1.15	0.88	**1.66**
185	28.3	16.9	Vcl	vinculin	15	43	0.84	1.25	**1.56**
186	27.8	37.5	Vim	Vimentin	19	60	1.10	0.79	**1.66**
238	24.3	42.0	Gap43	Neuromodulin	22	48	**5.97**	**3.77**	**5.01**
403	15.8	25.4	Tpm3	Isoform 1 of Tropomyosin alpha-3 chain [c]	8	18	**2.99**	**2.99**	**3.22**
Ubiquitin Proteosome System									
44	59.1	34.1	Ube1x	Ubiquitin-activating enzyme E1, Chr X	56	228	1.39	1.02	**1.74**
599	10.9	31.4	Uchl1	Ubiquitin carboxyl-terminal hydrolase isozyme L1	9	15	**2.81**	**1.85**	**1.77**
Nucleocytoplasmic Transport									
169	30.01	22.03	Kpnb1	Importin subunit beta-1	16	44	**1.33**	1.18	**1.50**
197	27.07	17.4	Ipo7	predicted importin 7 [d]	13	54	1.13	0.95	1.34
Housekeeping Gene (Control for WB, RT-PCR)									
40	60.09	39.9	Actn1	Brain-specific alpha actinin 1 isoform [c]	37	136	1.02	0.98	1.05

1

[a] These proteins have qualified through the pre-set selection criteria (i.e. unused prot score >2.0, *p*-value <0.05 for at least one ratio, magnitude of expression changes of at least 1.4 fold compared to the sham group), as mentioned in the "Results" section. They were classified according to their participation in the key molecular events of stroke pathophysiology. The ratios with significant *p*-value (<0.05) are shown in **bold**. [b] Proteins validated by WB. [c] Proteins whose of transcripts were measured by RT-PCR. [d] Proteins incorporated in the list due to their close association with the regulated proteins although they did not meet the above mentioned pre-set selection criteria. For example, Hk1, Ndufs1 and Ndufs2 (energy metabolism) are important enzymes of glucose catabolism. Pygm was the unperturbed muscle isoform of glycogen phosphorylase, whose brain isoform was significantly upregulated after 2 h MCAO. Similarly, Slc1a2, Glul, Slc16a1, Slc1a1 are related to glutamate neurotransmission and metabolism.

Figures

Figure 1.

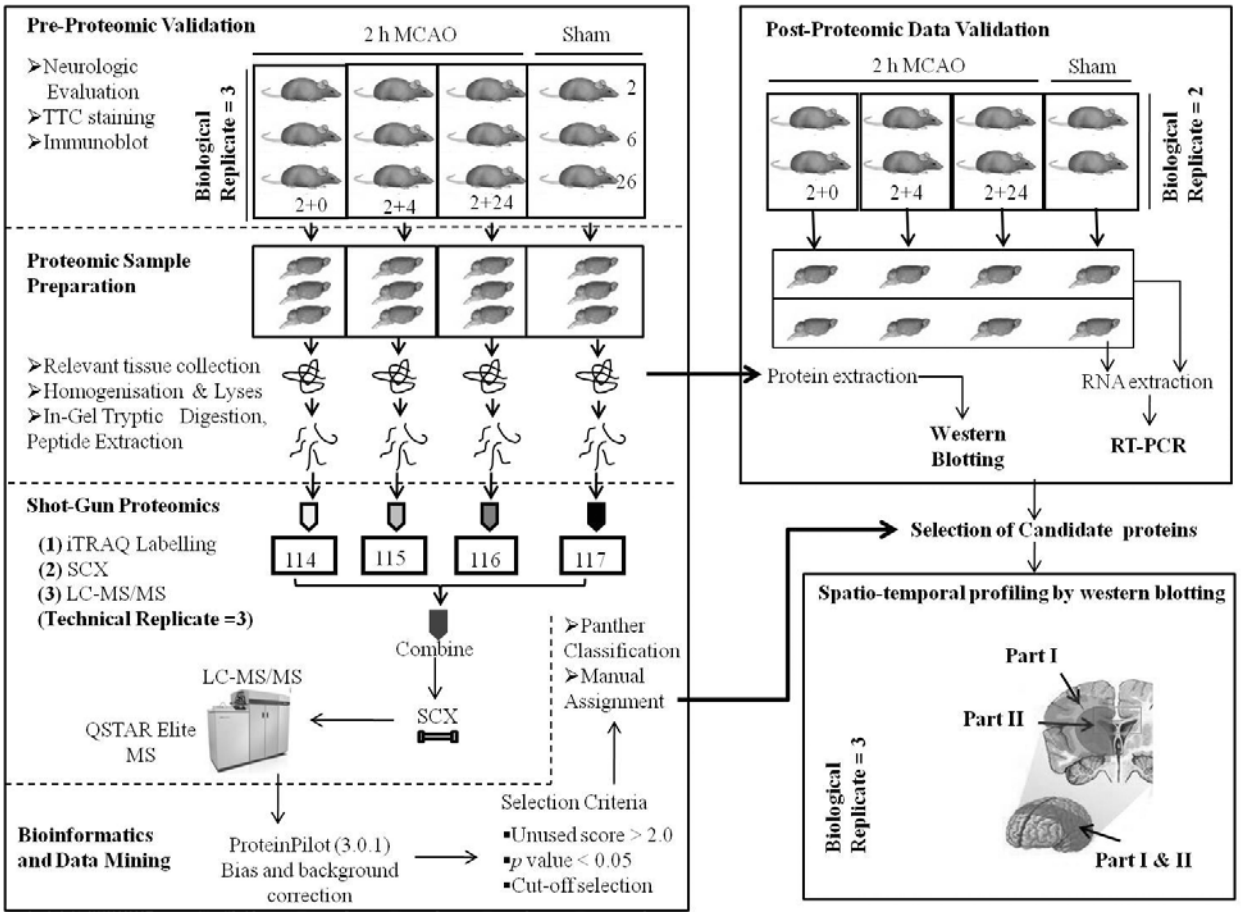

Figure 2.

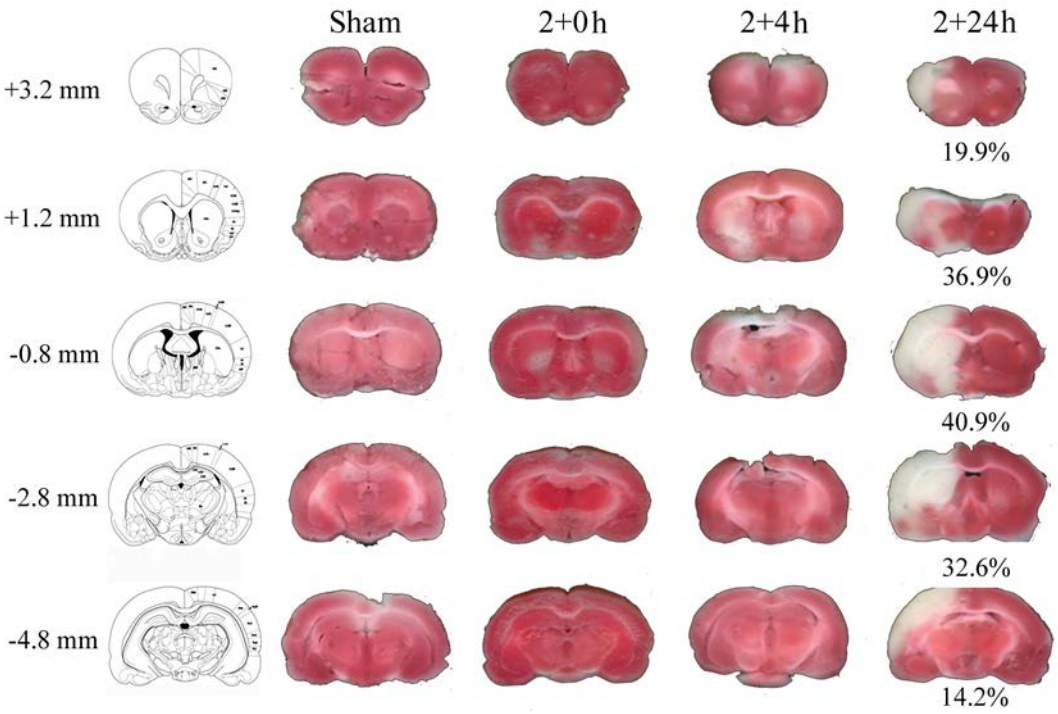

Figure 3.

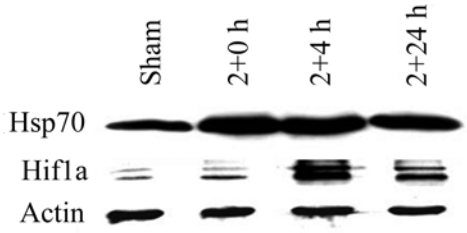

Figure 4.

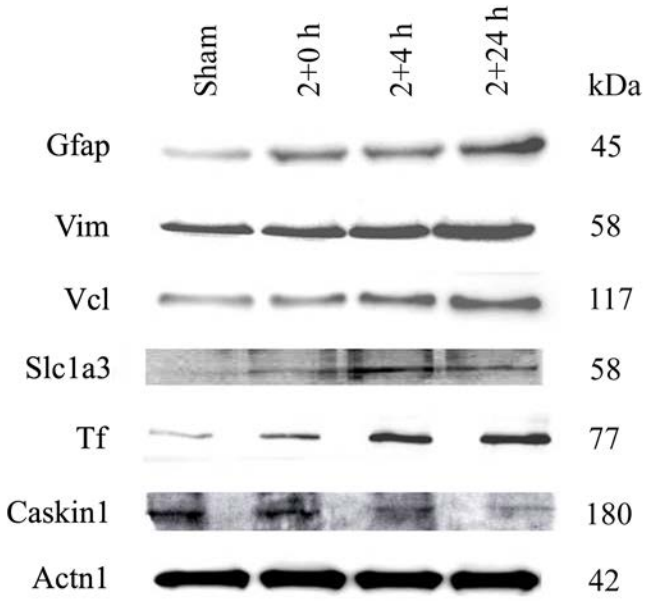

Figure 5.

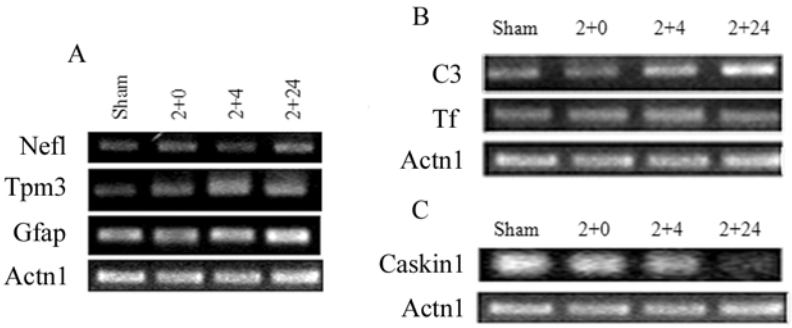

Figure 6.

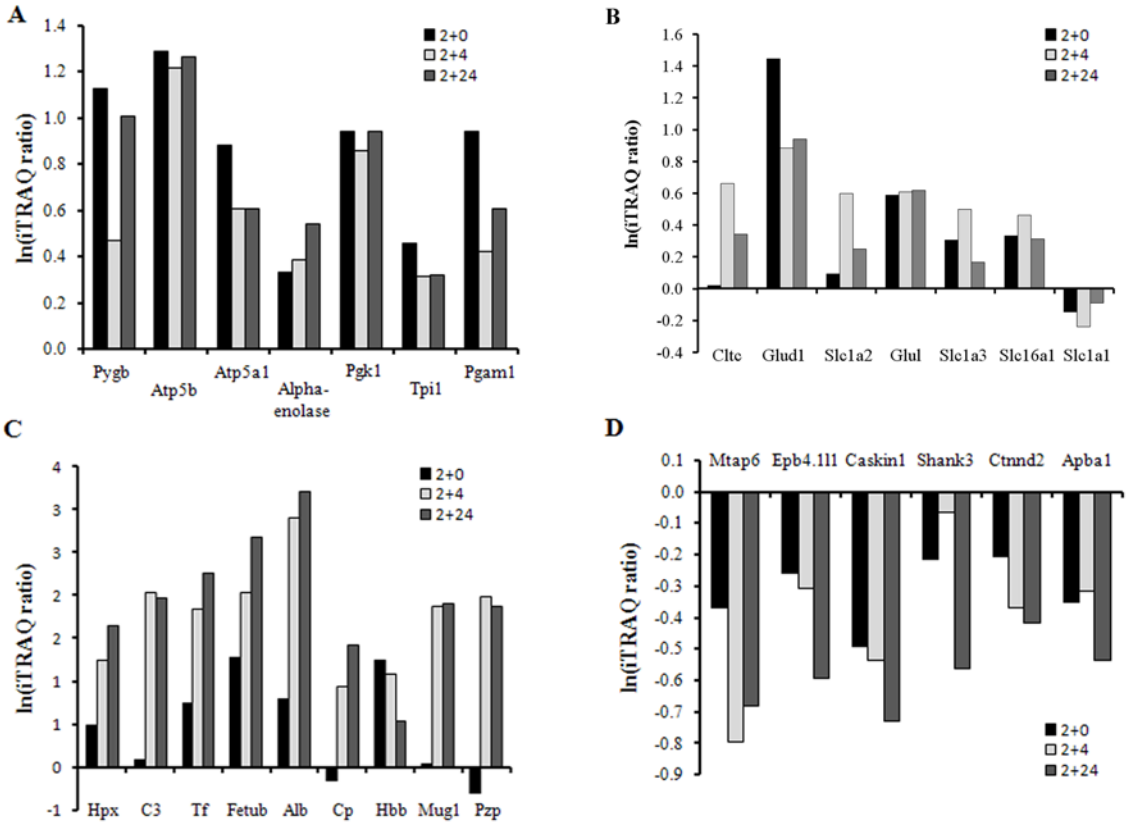

Figure 7.

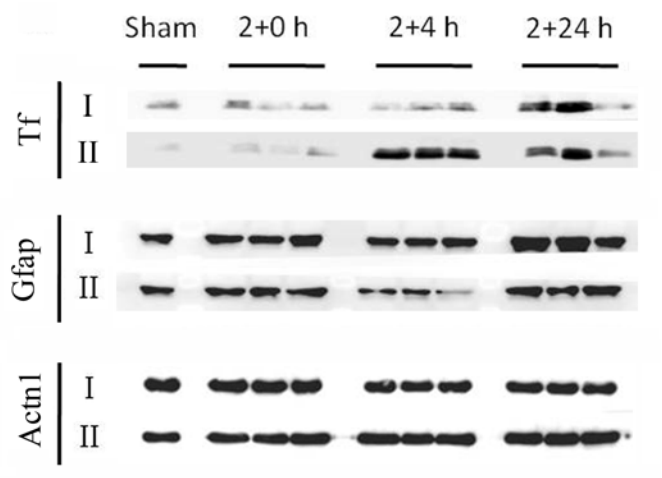

Figure 8.

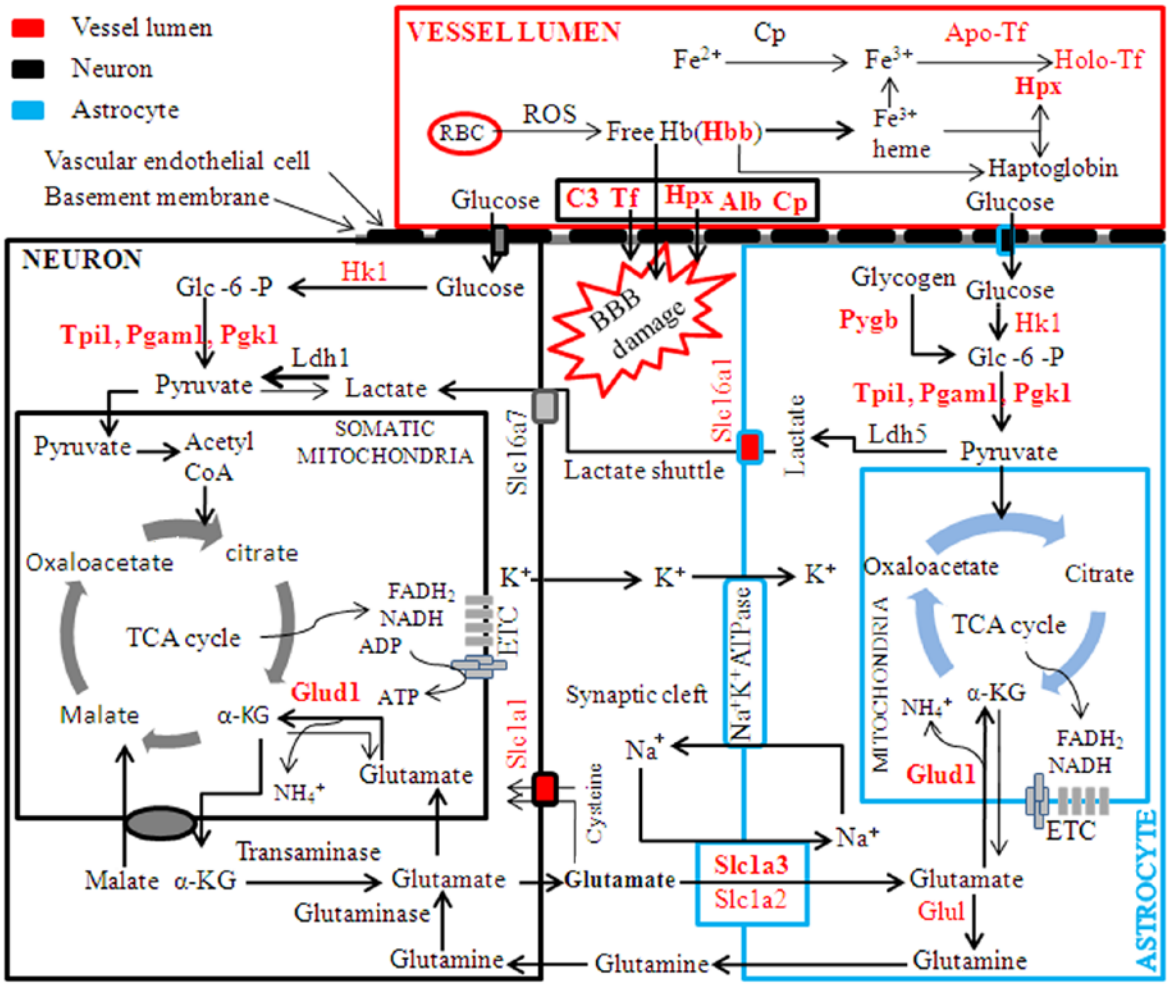

Location of Tables and Figures

Object	Suggested Location
Table 1	Page 8-9
Table 2	Page 15-16
Table 3	Page 21
Figure 1	Page 9
Figure 2	Page 16
Figure 3	Page 17
Figure 4	Page 20
Figure 5	Page 20
Figure 6	Page 22-23
Figure 7	Page 24
Figure 8	Page 27-33

Synopsis

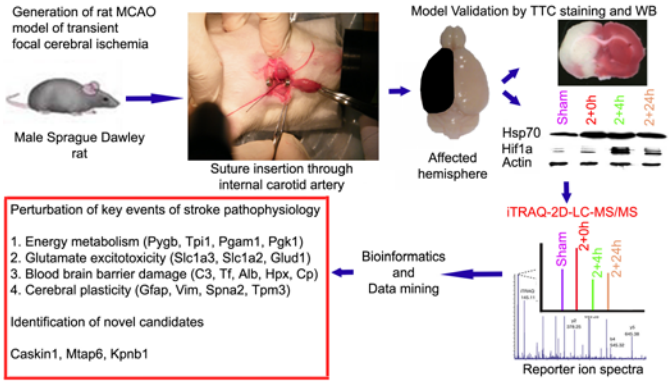

iTRAQ-2D-LC-MS/MS strategy was used to generate a temporal proteomics signature of the ischemic hemisphere in a MCAO model of cerebral ischemia-reperfusion injury. Data mining revealed, 1) active participation of astrocytes as a savior of neurons, 2) hyperacute opening of the blood brain barrier, and 3) late activation of a regenerative response. Discovery of Several regulated proteins (Caskin1 etc.) novel in context of stroke proved the utility of this shotgun neuroproteomics approach.